

A numerical study of the 1/2, 2/1 and 1/1 retrograde mean motion resonances in planetary systems

Gabriel Antônio Caritá,^{1*} Alan Cefali Signor,¹ Maria Helena Moreira Morais,^{1†}

¹*Instituto de Geociências e Ciências Exatas, Universidade Estadual Paulista (UNESP), Av. 24-A, 1515, 13506-900 Rio Claro, SP, Brazil*

Accepted 08 Jun 2022. Received 11 May 2022; in original form ZZZ

ABSTRACT

We present a numerical study on the stability of the 1/2, 2/1 and 1/1 retrograde mean motion resonances in the 3-body problem composed of a solar mass star, a Jupiter mass planet and an additional body with zero mass (elliptic restricted 3-body problem) or masses corresponding to either Neptune, Saturn or Jupiter (planetary 3-body problem). For each system we obtain stability maps using the n-body numerical integrator REBOUND and computing the chaos indicator *mean exponential growth factor of nearby orbits* (MEGNO). We show that families of periodic orbits exist in all configurations and they correspond to the libration of either a single resonant argument or all resonant arguments (fixed points). We compare the results obtained in the elliptic restricted 3-body problem with previous results in the literature and we show the differences and similarities between the phase space topology for these retrograde resonances in the circular restricted, elliptic restricted and planetary 3-body problems.

Key words: methods:numerical – planetary systems – chaos – planets and satellites: dynamical evolution and stability

1 INTRODUCTION

A retrograde resonance configuration occurs when 2 objects orbit a star in opposite directions and their orbital frequencies are commensurable (Morais & Giuppone 2012). The study of retrograde resonance in the framework of the circular restricted 3-body problem (Dobrovolskis 2012; Morais & Namouni 2013a; Namouni & Morais 2015; Morais & Namouni 2016b), allowed the identification of the first small bodies in retrograde resonances in the solar system, namely Centaurs in retrograde resonances with Jupiter and Saturn (Morais & Namouni 2013b) and asteroid (514107) Ka'epaoka'awela in the 1/1 (co-orbital) retrograde resonance with Jupiter (Wiegert et al. 2017; Morais & Namouni 2017; Namouni & Morais 2018). More recently, the families of periodic orbits which are associated with retrograde resonances have been computed in the spatial restricted 3-body problem (Morais & Namouni 2019; Kotoulas & Voyatzis 2020a; Morais et al. 2021; Kotoulas et al. 2022) and elliptic restricted 3-body problem (Kotoulas & Voyatzis 2020b,a; Kotoulas et al. 2022).

The possibility of retrograde resonances in extra-solar systems has been proposed by Gayon & Bois (2008); Gayon-Markt & Bois (2009) but no exhaustive studies on the stability of such configurations had been conducted until now. The formation of systems with counter-revolving planets is possible e.g. due to close encounters between stars leading to exchange of planets between them (Malmberg et al. 2011). These captured planets may have high inclination orbits with respect to the ones that formed in situ.

In this article we present a numerical investigation of retrograde resonances in the planar planetary three body problem using stability

and resonance maps. In Sect. 2 we explain our numerical search methodology and we present results for the retrograde resonances 1/2, 2/1 and 1/1 in the elliptic and planetary three body problems. In Sect. 3 we discuss these results and in Sect. 4 we present our conclusions.

2 NUMERICAL STUDY OF RETROGRADE MEAN MOTION RESONANCES

We consider the three body problem composed of a solar mass star and two planets orbiting the star in opposite directions, one counter-clockwise (prograde) and the other clockwise (retrograde). We use the notation $p/-q$ mean motion resonance to refer to a configuration where 2 planets orbiting the star in opposite directions have mean motions (average orbital frequencies) which are nearly commensurable in the the ratio p/q (Morais & Namouni 2013a). We use the usual notation for astrometric orbital elements: a (semi-major axis), T (orbital period), e (eccentricity), I (inclination), M (mean anomaly), ω (argument of pericenter), Ω (longitude of ascending node), λ (mean longitude), ϖ (longitude of pericenter). Variables with subscript p refer to the prograde planet and those without subscript refer to the retrograde planet. The prograde planet has mass $0.001 M_{\odot}$ and the unit distance is its mean distance to the star, i.e. $a_p = 1$. In the elliptic restricted 3-body problem (ER3BP) the retrograde planet has zero mass, and in the planetary 3-body problem it has mass equal to either Neptune ($0.00005149 M_{\odot}$), Saturn ($0.0002857 M_{\odot}$) or Jupiter ($0.001 M_{\odot}$). We investigate the stable configurations of planar systems in the 1/-2, 2/-1 and 1/-1 mean motion resonances.

The numerical integration of the equations of motion were performed using REBOUND with the adaptive step integrator IAS15 (Rein & Spiegel 2015) and in some cases (especially high eccentric-

* E-mail: gabrielcarita@gmail.com

† E-mail: helena.morais@unesp.br

ity orbits) using the Bulirsch-Stoer method implemented in MERCURY (Chambers 1999). The integration for a particular object was stopped when the mutual distance to another object was smaller than the sum of their radii (collision) or when the distance to the star was larger than $10 a_p$ (escape).

We assume a counter-clockwise reference frame. The longitudes defined in the orbital plane for the prograde planet (with counter-clockwise motion) are measured in the direction of the object's orbital motion, hence $\lambda_p = \Omega_p + \omega_p + M_p$, $\varpi_p = \Omega_p + \omega_p$, while those for the retrograde planet (with clockwise motion) are measured against the direction of the object's orbital motion, hence $\lambda = \Omega - \omega - M$, $\varpi = \Omega - \omega$. This is also the convention used within REBOUND.

We construct stability and resonant maps. The stability maps are obtained by computation of the chaotic indicator MEGNO, which converges to 2 for stable orbits while values greater than 2 indicate chaos (Cincotta & Simó 2000; Goździewski 2003). The resonant maps indicate regions of libration of the resonant angle of the circular restricted 3-body problem which for a $p/-q$ mean motion resonance is $\phi_0 = -q\lambda - p\lambda_p + (p+q)\varpi$ (Morais & Namouni 2013a). There are also regions of libration of both ϕ_0 and $\varpi - \varpi_p$ (which indicates a fixed point of the resonant problem), identified by a white symbol. Regions of libration of a single resonant argument different from ϕ_0 (which we will define shortly for each resonance) are identified by a black symbol. The color bar in the resonant maps indicates the semi-amplitude of ϕ_0 libration i.e. the maximum variation around the resonant center. We identify fixed points when both ϕ_0 and $\varpi - \varpi_p$ librate (around either 0 or π) with semi-amplitude less than $\pi/4$.

We construct 2 types of maps: 1) eccentricity of the prograde planet versus eccentricity of the retrograde planet with initial semi-major axis fixed at the nominal resonance location $a = (q/p)^{2/3}$; 2) eccentricity versus semi-major axis of the retrograde planet at fixed initial prograde planet's eccentricity. In 1) we used a grid of 80×80 initial eccentricities in the range $[0, 1]$ while in 2) we have initial (a, e) in a 40×40 (low resolution) or 80×80 grid (high resolution). In both cases we integrated for $2 \times 10^5 T_p$.

We set the initial longitudes of the nodes to be zero ($\Omega = \Omega_p = 0$). The initial inclination of the retrograde planet with respect to the prograde planet's orbital plane is set to $I = 179.99^\circ$. In some cases we will see differences between this nearly-coplanar case with results presented for strictly 2D cases (where the zed components of the positions and velocities of all objects are strictly zero). In practice this means that such 2D periodic orbits are vertically unstable and will not exist in real systems. Therefore, integrating the nearly coplanar case is more relevant for studying the dynamics of real systems which will never be exactly coplanar.

We investigate all possible permutations of aligned / anti-aligned pericenters / apocenters separated by quadrants displayed in Figure 1. In Q_1 , $\varpi_p = \varpi = 0$; in Q_2 , $\varpi_p = 0$, $\varpi = \pi$; in Q_3 , $\varpi_p = \varpi = \pi$; in Q_4 , $\varpi_p = \pi$, $\varpi = 0$. The initial mean anomaly of the prograde planet is $M_p = \varpi_p$, while the mean anomaly of the retrograde body is $M = 0$ (Figure 1 (a)), or $M = \pi$ (Figure 1 (b)). The Roman numerals indicate pairing of initial configurations which, due to the commensurability between the orbital periods, are equivalent with a time-lag of half a period of the external object. This equivalence is not exact due to the interaction between the planets during that time-lag.

2.1 1/2 Resonance

For resonance 1/2 the resonant angles analyzed were:

$$\phi_0 = -2\lambda - \lambda_p + 3\varpi \quad (1)$$

$$\phi_1 = -2\lambda - \lambda_p + 3\varpi_p \quad (2)$$

$$\phi_2 = -2\lambda - \lambda_p + 2\varpi_p + \varpi \quad (3)$$

$$\phi_3 = -2\lambda - \lambda_p + \varpi_p + 2\varpi \quad (4)$$

Table 1 presents the summarized results of the 1/2 resonant configurations, indicating the object's masses and libration angles.

In Figure 2 for $M = 0$ (a) and $M = \pi$ (b) we present the results for the ER3BP. The color bar indicates the amplitude of the resonant angle ϕ_0 , where dark purple/blue indicates the resonance center. In the 1st quadrant (Q_1) of the both maps there are periodic families where ϕ_0 and $\varpi - \varpi_p$ (hence also ϕ_1, ϕ_2, ϕ_3) librate simultaneously (fixed point families) which we represent by overlaying white symbols in the darker region. From Figure 1 we expect approximate symmetry between the quadrants in Figure 2 (a) and (b). In fact, we see the same structures in both panels but for $M = \pi$ the fixed point family in Q_1 has decreased while the ϕ_0 family has increased in quadrants Q_2, Q_3 and Q_4 , in comparison with $M = 0$.

The 1/2 resonance at Jupiter to Sun mass ratio in the CR3BP was studied in Morais & Namouni (2016a). In that work the $\phi_0 = 0$ family starts at $e > 0.4$ in agreement with our results (purple regions at $e_p = 0$ on right hand side of 2 (a) and (b)), while the $\phi_0 = \pi$ exists from $e = 0$ up to $e \approx 0.8$ also in agreement with our results (purple regions at $e_p = 0$ on left hand side of 2 (a) and (b)). The 1/2 resonance was also studied in the ER3BP at Neptune to Sun mass ratio in Kotoulas & Voyatzis (2020a). The fixed point family which appears in the ER3BP at Jupiter to Sun mass ratio family (1st quadrants of 2 (a) and (b)) is qualitatively in agreement with the stable family computed by Kotoulas & Voyatzis (2020a).

The stability maps for the planetary problem when the second planet has Neptune's mass, are presented Figure 3. We can observe the same resonant families present in the ER3BP, however, a new fixed point resonance region appears in the first quadrant, near $e_p = 0.05$. This happens for both cases $M = 0$ and $M = \pi$. In Figure 4 we show the orbital evolution corresponding to the initial conditions marked with red circles in Figure 3. In both cases all resonant angles and $\varpi - \varpi_p$ librate around 0 with small amplitude as expected for a fixed point resonant family.

The stability maps for the planetary problem when the 2nd planet has Saturn's mass are presented in Figure 5. The fixed point family of the ER3BP is still present in Q_1 while the additional fixed point family within the $\phi_0 = 0$ libration region which was observed when the 2nd planet has Neptune's mass is displaced to larger e_p . There is another fixed point family which appears in Q_3 at $e_p \approx 0$ within the $\phi_0 = \pi$ libration region. In Q_1 and Q_2 a new family appears which corresponds to libration of ϕ_3 only (represented by black overlaying symbols).

The stability maps for the planetary problem when the 2nd planet has Jupiter's mass are presented in Figure 6 for $M = 0$ and $M = \pi$. The resonant families in this case are qualitatively similar to the ones present in Figure 5 but with the difference that libration of ϕ_0 only is absent in the case of 2 jovian planets. In Figure 7 we show the orbital

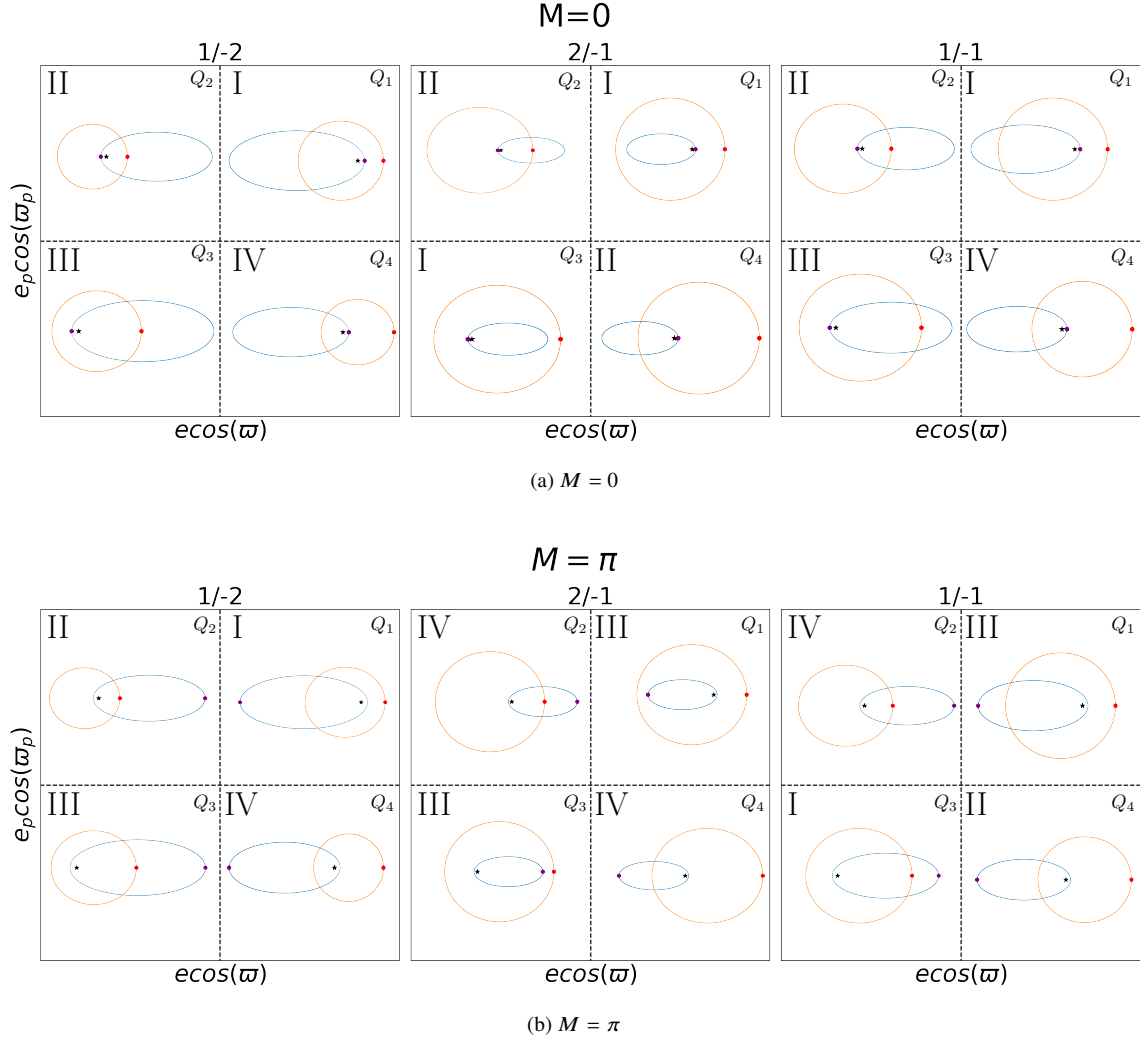
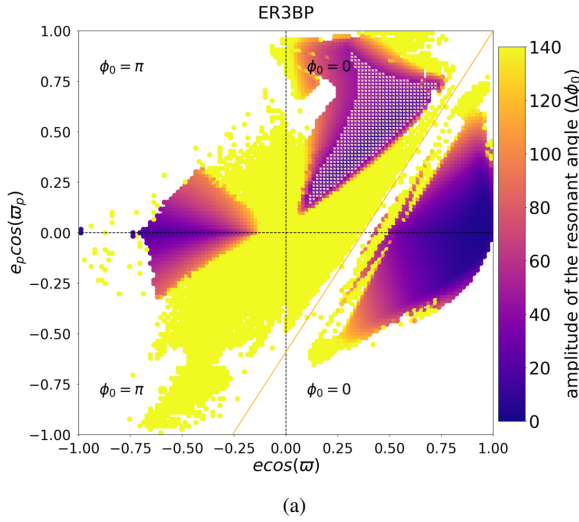


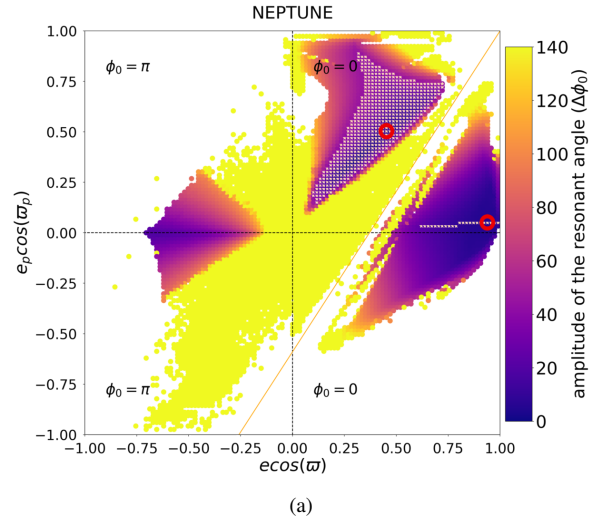
Figure 1. Configurations displayed in 4 quadrants which represent the initial orientations of the pericenters / apocenters, and initial conditions $M_P = \varpi_P$ and $M = 0$ (a) or $M = \pi$ (b). The Roman numerals indicate pairing of initial configurations which, due to the commensurability between the orbital periods, are equivalent with a time-lag of half a period of the external object.

Table 1. Table reporting the summarized results for the 1/-2 resonance. The notation $\phi_{0,1,2,3}$ indicates fixed point libration (ϕ_0 and $\varpi - \varpi_P$ are fixed), and either ϕ_0 or ϕ_3 indicates libration of a single angle.

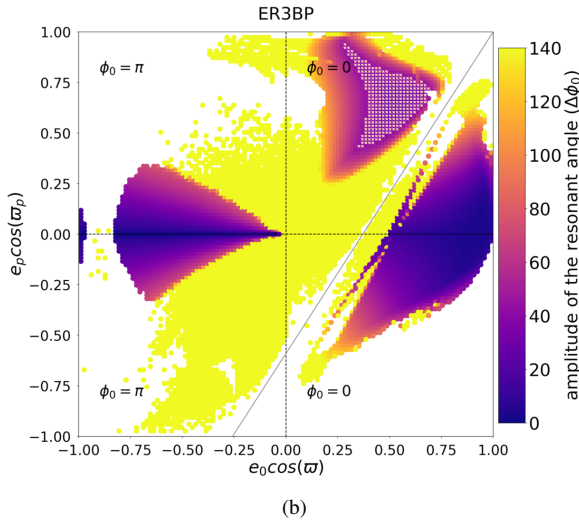
Mass	Resonance				Figure
	Q_1	Q_2	Q_3	Q_4	
ER3BP($M = 0$)	$\phi_{0,1,2,3}$ and ϕ_0	ϕ_0	ϕ_0	ϕ_0	2a
ER3BP($M = \pi$)	$\phi_{0,1,2,3}$ and ϕ_0	ϕ_0	ϕ_0	ϕ_0	2b
NEPTUNE($M = 0$)	$\phi_{0,1,2,3}$ and ϕ_0	ϕ_0	ϕ_0	ϕ_0	3a
NEPTUNE($M = \pi$)	$\phi_{0,1,2,3}$ and ϕ_0	ϕ_0	ϕ_0	ϕ_0	3b
SATURN($M = 0$)	$\phi_{0,1,2,3}$ and ϕ_3	ϕ_0 and ϕ_3	$\phi_{0,1,2,3}$	ϕ_0	5a
SATURN($M = \pi$)	$\phi_{0,1,2,3}$ and ϕ_3	ϕ_0 and ϕ_3	$\phi_{0,1,2,3}$	ϕ_0	5b
JUPITER($M = 0$)	$\phi_{0,1,2,3}$ and ϕ_3	ϕ_3	$\phi_{0,1,2,3}$	-	6a
JUPITER($M = \pi$)	$\phi_{0,1,2,3}$ and ϕ_3	ϕ_0 and ϕ_3	$\phi_{0,1,2,3}$ and ϕ_0	-	6b



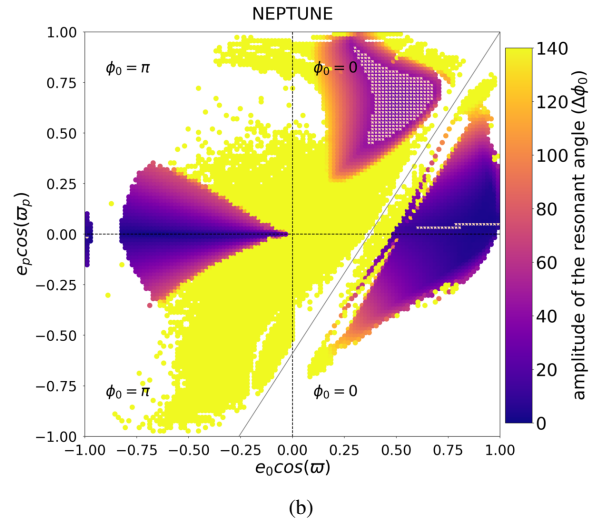
(a)



(a)



(b)



(b)

Figure 2. Resonant maps for the 1/2 resonance in the elliptic restricted three body problem (a) $M = 0$; (b) $M = \pi$. The color bar represents the amplitude of the restricted angle ($\Delta\phi_0$) and the overlaying white symbols indicate the fixed point family where all resonant angles librate around a center. The orange and gray lines indicate collision at time zero or after half a period of the external object, respectively.

evolution corresponding to the initial conditions marked with red circle in Figure 6 ($e = 0.49$, $e_p = 0.48$). In this case ϕ_3 is the only angle librating while the others are circulating. The eccentricities of both bodies exhibit simultaneous periodic variations with larger amplitude for the prograde planet.

2.2 2/-1 Resonance

For the retrograde resonance 2/1 the resonant angles analyzed were:

$$\phi_0 = -\lambda - 2\lambda_p + 3\varpi \quad (5)$$

$$\phi_1 = -\lambda - 2\lambda_p + 3\varpi_p \quad (6)$$

$$\phi_2 = -\lambda - 2\lambda_p + \varpi_p + 2\varpi \quad (7)$$

Figure 3. Resonant maps for the 1/2 resonance in the planetary problem when the 2nd planet has Neptune's mass (a) $M = 0$; (b) $M = \pi$. The color bar represents the amplitude of the restricted angle ($\Delta\phi_0$) and the overlaying white symbols indicate the fixed point family where all resonant angles librate around a center. The orange and gray lines indicate collision at time zero or after half a period of the external object, respectively.

$$\phi_3 = -\lambda - 2\lambda_p + 2\varpi_p + \varpi \quad (8)$$

Table 2 presents the summarized results of the 2/-1 resonant configurations, indicating the object's masses and libration angles.

The stability maps for the ER3BP are presented in Figure 8 for $M = 0$ (a) and $M = \pi$ (b). The color bar indicates the amplitude of the resonant angle ϕ_0 , where dark purple/blue indicates the resonance center. The top panel (a) corresponds to the resonant center $\phi_0 = 0$ while the bottom panel (b) corresponds to the resonant center $\phi_0 = \pi$. From Figure 1 we expect approximate symmetry between the quadrants Q_1 and Q_3 , Q_2 and Q_4 at fixed $M = 0$ or $M = \pi$, which we indeed observe in Figure 8 (a) and (b). There are fixed point families in the four quadrants for $M = 0$: 2 large islands in Q_1 and Q_3 and 2 smaller islands in Q_2 and Q_4 . There are regions where there is libration of the angle ϕ_0 near $e_p = 0$ on the left and right of panel (a), and a few points in Q_1 and Q_3 that correspond to libration

Table 2. Table reporting the summarized results for the 2/-1 resonance. The notation $\phi_{0,1,2,3}$ indicates fixed point libration (ϕ_0 and $\varpi - \varpi_p$ are fixed), and either ϕ_0 or ϕ_3 indicates libration of a single angle.

Mass	Resonance				Figure
	Q_1	Q_2	Q_3	Q_4	
ER3BP($M = 0$)	$\phi_{0,1,2,3}, \phi_0$ and ϕ_3	$\phi_{0,1,2,3}, \phi_0$ and ϕ_3	$\phi_{0,1,2,3}, \phi_0$ and ϕ_3	$\phi_{0,1,2,3}, \phi_0$ and ϕ_3	8a
ER3BP($M = \pi$)	$\phi_{0,1,2,3}$	-	$\phi_{0,1,2,3}$	-	8b
NEPTUNE($M = 0$)	$\phi_{0,1,2,3}, \phi_0$ and ϕ_3	$\phi_{0,1,2,3}, \phi_0$ and ϕ_3	$\phi_{0,1,2,3}, \phi_0$ and ϕ_3	$\phi_{0,1,2,3}, \phi_0$ and ϕ_3	9a
NEPTUNE($M = \pi$)	$\phi_{0,1,2,3}$	-	$\phi_{0,1,2,3}$	-	9b
SATURN($M = 0$)	$\phi_{0,1,2,3}$ and ϕ_3	ϕ_0 and ϕ_3	$\phi_{0,1,2,3}$ and ϕ_3	ϕ_0 and ϕ_3	11a
SATURN($M = \pi$)	$\phi_{0,1,2,3}$	-	$\phi_{0,1,2,3}$	-	11b
JUPITER($M = 0$)	$\phi_{0,1,2,3}$ and ϕ_3	ϕ_3	$\phi_{0,1,2,3}$ and ϕ_3	$\phi_{0,1,2,3}, \phi_0$ and ϕ_3	12a
JUPITER($M = \pi$)	$\phi_{0,1,2,3}$	-	$\phi_{0,1,2,3}$	-	12b

of the angle ϕ_3 . For $M = \pi$ there are fixed point families in quadrants Q_1 and Q_3 .

The 2/-1 resonance at Jupiter to Sun mass ratio in the CR3BP was studied in [Morais & Namouni \(2016a\)](#) and [Kotoulas & Voyatzis \(2020b\)](#). According to these works, the $\phi_0 = 0$ is present at nearly all values of e in agreement with our results (purple regions at $e_p = 0$ on right and left hand sides of Figure 8 (a)), while the $\phi_0 = \pi$ exists from $e > 0.6$ in the planar problem when $e_p = 0$. This latter family does not appear in Figure 8 (b) because it is vertically unstable ([Kotoulas & Voyatzis 2020b](#)). As we integrate the 3D equations of motion, our problem is not strictly 2D and therefore we do not recover vertically unstable families. In practice, strictly planar systems do not exist hence we do not expect to find real systems in resonant configurations which are vertically unstable. The 2/-1 resonance at Jupiter to Sun mass ratio was also studied in the ER3BP by [Kotoulas & Voyatzis \(2020b\)](#). Our results are in agreement regarding the fixed point point families at in Figure 8 (a). However the fixed point point families in Figure 8 (b) have not been reported by [Kotoulas & Voyatzis \(2020b\)](#).

The stability maps for the planetary problem when the 2nd planet has Neptune's mass are presented in Figure 9. At $e_p \approx 0$ on the left and right hand side of panel (a) there are now 2 fixed point families, corresponding to configurations where the pericenters are aligned (in Q_1 and Q_3) or anti-aligned (in Q_2 and Q_4). The latter family was already present in the ER3BP. The family associated with the 2 large fixed point regions in Q_1 and Q_3 is nearly identical to the family observed in the ER3BP. There are also 4 regions distributed in the 4 quadrants where the angle ϕ_2 librates. It's clear the symmetry between Q_1 and Q_2 , and also Q_3 and Q_4 . For $M = \pi$ we obtain the exactly the same structures that observed in ER3BP: two fixed resonance families at large e_p in Q_1 and Q_3 . In Figure 10 we show the orbital evolution corresponding to the initial conditions marked with red circle in Figure 9. In this case all resonant angles and $\varpi - \varpi_p$ librate around either 0 or π with small amplitude as expected for a fixed point resonant family.

The stability maps for the planetary problem when the 2nd planet has Saturn's mass are presented in Figure 11. In Figure 11 (a) ($M = 0$) the main difference from the case when the 2nd planet has Neptune's mass is the destruction of the fixed point region near $e_p = 0$ at large e . In Figure 11 (b) ($M = \pi$) we see that the fixed point family at large e_p in Q_1 and Q_3 is reduced with respect to the ER3BP and the case of a 2nd planet with Neptune's mass.

The stability maps for the planetary problem when the 2nd planet has Jupiter's mass are presented in Figure 12. In Figure 12 (a) we observe the same structures already described in the case where the 2nd planet has Saturn's mass. However, although we expect mirroring of the resonant structures observed in Q_1 and Q_3 , and also in Q_2 and Q_4 , as the initial conditions in these configurations are approximately

equivalent with a time lag equal to half a period of the external body (Figure 1), it is now clear that there is no exact symmetry. This is due to the non negligible interaction between the 2 jovian planets during that time lag which implies that the configurations are not exactly equivalent. In particular, there is a small fixed point family in quadrant Q_4 near $e_p = 0.75$ which is not present in Q_2 . In Q_1 and Q_3 of Figure 12 (b) the fixed point family present at smaller masses of the 2nd planet does no longer exist but there are 2 new fixed point small islands.

In Figure 13 we show the orbital evolution corresponding to the initial condition marked with red circle in Q_1 of Figure 12 (a). In this case only the resonant angle ϕ_2 librates while all other resonant angles circulate. Unlike the behavior observe in 1/-2 resonance, in 2/-1 resonance the amplitude of the eccentricity of the retrograde planet is higher than the prograde body. In Figure 14, we show the orbital evolution corresponding to the initial condition marked with red circle in Q_4 of Figure 12 (a). In this case there is a fixed point resonance where ϕ_1 and ϕ_3 librate around 0 while ϕ_0 and ϕ_2 around π . Figure 15 shows that the initial condition marked with red circle in Q_1 of Figure 12 (b), corresponds to a fixed point resonance.

2.3 1/-1 resonance

For resonance 1/-1 the resonant angles analyzed were:

$$\phi_0 = -\lambda - \lambda_p + 2\varpi \quad (9)$$

$$\phi_1 = -\lambda - \lambda_p + 2\varpi_p \quad (10)$$

$$\phi_2 = -\lambda - \lambda_p + \varpi_p + \varpi \quad (11)$$

Table 3 presents the summarized results of the 1/-1 resonant configurations, indicating the object's masses and libration angles.

The stability maps for the ER3BP are presented in Figure 16 for $M = 0$ (a) and $M = \pi$ (b). The color bar indicates the amplitude of the resonant angle ϕ_0 , where dark purple/blue indicates the resonance center. The top panel (a) corresponds to $M = 0$, which implies $\phi_0 = 0$ in Q_1, Q_4 , and $\phi_0 = \pi$ in Q_2, Q_3 , while the bottom panel (b) corresponds to $M = \pi$, which implies $\phi_0 = \pi$ in Q_1, Q_4 , and $\phi_0 = 0$ in Q_2, Q_3 . From Figure 1 we expect approximate symmetry between Q_1 (Q_3) at $M = 0$ and Q_3 (Q_1) at $M = \pi$, and also between Q_2 (Q_4) at $M = 0$ and Q_4 (Q_2) at $M = \pi$. However, it is again clear that this symmetry is not exact. In this case we did not observe fixed point families for $M = 0$. We have obtained fixed families for $M = \pi$ in Q_1 and Q_4 , however these families occur when the planet's

Table 3. Table reporting the summarized results for the 1/-1 resonance. The notation $\phi_{0,1,2}$ indicates fixed point libration (ϕ_0 and $\varpi - \varpi_p$ are fixed), while ϕ_0 indicates libration of the CR3BP angle.

Mass	Resonance				Figure
	Q_1	Q_2	Q_3	Q_4	
ER3BP($M = 0$)	ϕ_0	ϕ_0	ϕ_0	ϕ_0	16a
ER3BP($M = \pi$)	$\phi_{0,1,2}$ and ϕ_0	ϕ_0	ϕ_0	$\phi_{0,1,2}$ and ϕ_0	16b
NEPTUNE($M = 0$)	$\phi_{0,1,2}$ and ϕ_0	ϕ_0	ϕ_0	ϕ_0	17a
NEPTUNE($M = \pi$)	$\phi_{0,1,2}$ and ϕ_0	ϕ_0	$\phi_{0,1,2}$	$\phi_{0,1,2}$ and ϕ_0	17b
SATURN($M = 0$)	ϕ_0	ϕ_0	ϕ_0	-	18a
SATURN($M = \pi$)	$\phi_{0,1,2}$	ϕ_0	ϕ_0	ϕ_0	18b
JUPITER($M = 0$)	-	-	$\phi_{0,1,2}$	-	20a
JUPITER($M = \pi$)	$\phi_{0,1,2}$	-	-	-	20b

eccentricity, e_p , is near 1 and thus their long term stability requires further investigation. Moreover, the region corresponding to $\phi_0 = \pi$ libration at large eccentricity e , is wider when $M = \pi$ (Figure 16 (b)) than when $M = 0$ (Figure 16 (a)).

The 1/-1 resonance at Jupiter to Sun mass ratio in the CR3BP was studied in [Morais & Namouni \(2016b, 2019\)](#). There are 2 planar resonant modes: $\phi_0 = 0$ which is stable when $e > 0.1$ and whose center occurs at the nominal resonance location, $a = 1$, when $e > 0.5$ in agreement with our results (purple regions at $e_p = 0$ on right hand side of Figure 16 (a) and left hand side of Figure 16 (b)); $\phi_0 = \pi$ which occurs at the nominal resonant location $a = 1$ when $e > 0.75$ also in agreement with our results (purple regions at $e_p = 0$ on left hand side of Figure 16 (a) and right hand side of Figure 16 (b)).

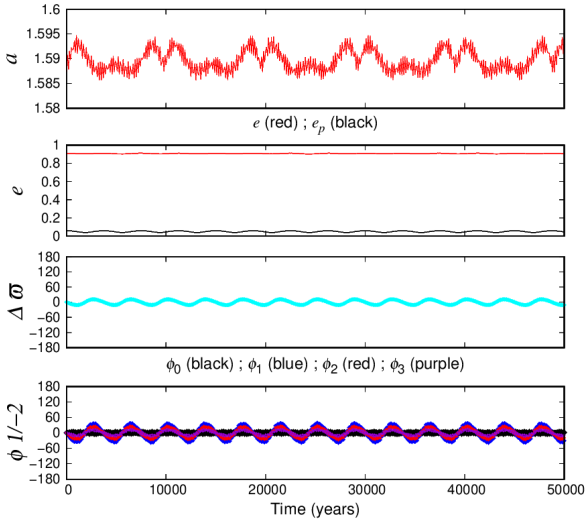
The stability maps for the planetary problem when the 2nd planet has Neptune's mass are presented in Figure 17. At the center of ϕ_0 family of the ER3BP there is now a fixed point family near $e_p = 0$ seen on right side of Figure 17 (a) and left side of Figure 17 (a). Although this fixed point family appears to have gaps in Figure 17, a zoom of this region with a higher resolution grid shows that it is in fact a continuous family.

The stability maps for the planetary problem when the 2nd planet has Saturn's mass are presented in Figure 18. At the nominal resonance location $a = 1$ we only obtain stable solutions with $\phi_0 = \pi$ at large e . When $e_p \approx 0$ there is a fixed point family at the center of the $\phi_0 = \pi$ region which appears with starting $M = \pi$ (Figure 18 (b)) but not $M = 0$ (Figure 18 (a)). Figure 19 shows the stability map in Q_1 for the planetary problem when the 2nd planet has Saturn's mass, with initial conditions $a = 1.01$, $M = 0$, $\varpi = \varpi_p = 0$ (hence $\phi_0 = 0$). The fixed point family in this case is displaced from the nominal resonance location.

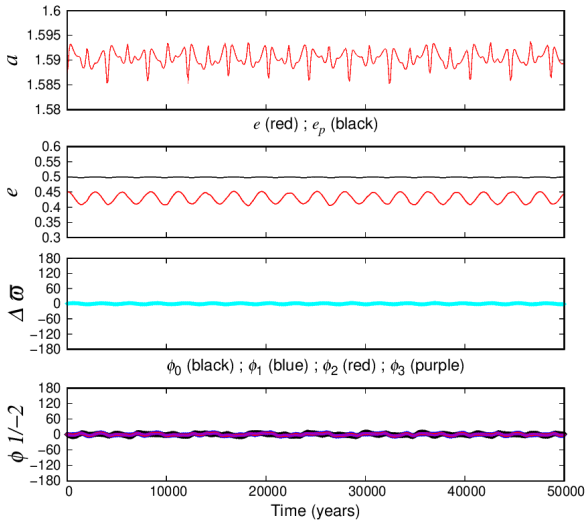
The stability maps for the planetary problem when the 2nd planet has Jupiter's mass are presented in Figure 20. In this case the stable islands are associated with fixed point families which occur for the initial angle $\phi_0 = \pi$ seen in Q_3 in Figure 20 (a) and in Q_1 in Figure 20 (b), while most other initial conditions lead to collision or escape. Figure 21 shows the orbital evolution of the initial condition marked by red circle in Figure 20 (b) ($e_0 = 0.94$, $e_p = 0.47$). The stability islands above and below the collision line at fixed $M = 0$ or $M = \pi$ in 20 are not exactly symmetric (as we would expect as inverting the direction of motion of both planets results in the same relative motion) since they correspond to initial conditions with a time-lag of half a period (Figure 1). This also explains the mirrored structures in quadrants Q_3 (Figure 20 (a)) and Q_1 (Figure 20 (a)).

We present (a, e) stability maps in Figure 22 using initial condi-

tions from Figure 20. In this case, the color bar indicates the MEGNO value of the system, being stable blue/purple and unstable yellow, and the integration time span is $2 \times 10^5 T_p$. In 22 (a) we fix $e_p = 0.9$ in order to explore the smaller fixed point island in Figure 20 (b). We see that in this case there are 2 branches of the fixed point family, one at $a = 1$, and the other at $a \approx 1.03$. In 22 (a) we fix $e_p = 0.4$ in order to explore the larger fixed point island in Figure 20 (b). In this case the fixed point family is centered at $a = 1$.

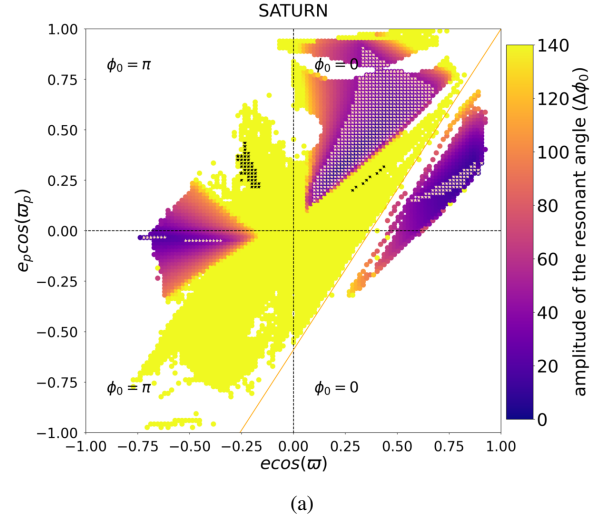


(a)

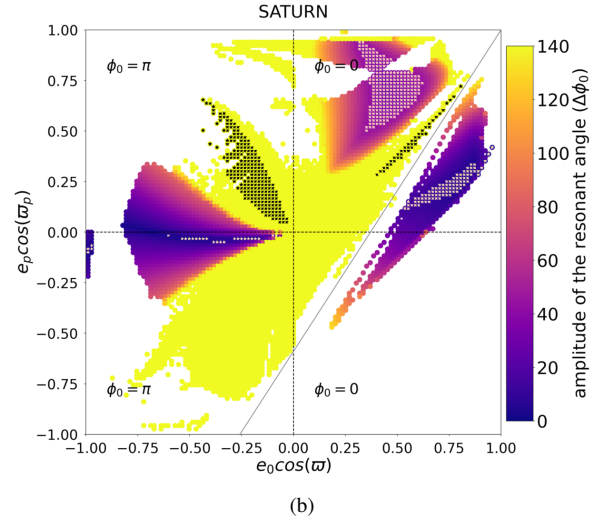


(b)

Figure 4. Orbital evolution as a function of time for the initial conditions circled in Figure 3a ($Q_1, M = 0$). In (a) the initial conditions are $e = 0.91$ and $e_p = 0.058$. In (b) the initial conditions are $e = 0.45$, $e_p = 0.5$. In (a) and (b) the 1st panel shows the semi-major axis of the third body, the 2nd panel shows its orbital eccentricity, the 3rd panel shows the difference $\Delta\omega$ between the longitudes of pericenter, the 4th panel shows the resonant angles ϕ_0 , ϕ_1 , ϕ_2 , and ϕ_3 .



(a)



(b)

Figure 5. Resonant maps for the 1/-2 resonance in the planetary problem when the 2nd planet has Saturn's mass (a) $M = 0$; (b) $M = \pi$. The color bar represents the amplitude of the restricted angle ($\Delta\phi_0$) and the overlaying white symbols indicate the fixed point family where all resonant angles librate around a center. The black symbols indicate libration of ϕ_3 only. The orange and gray lines indicate collision at time zero or after half a period of the external object, respectively.

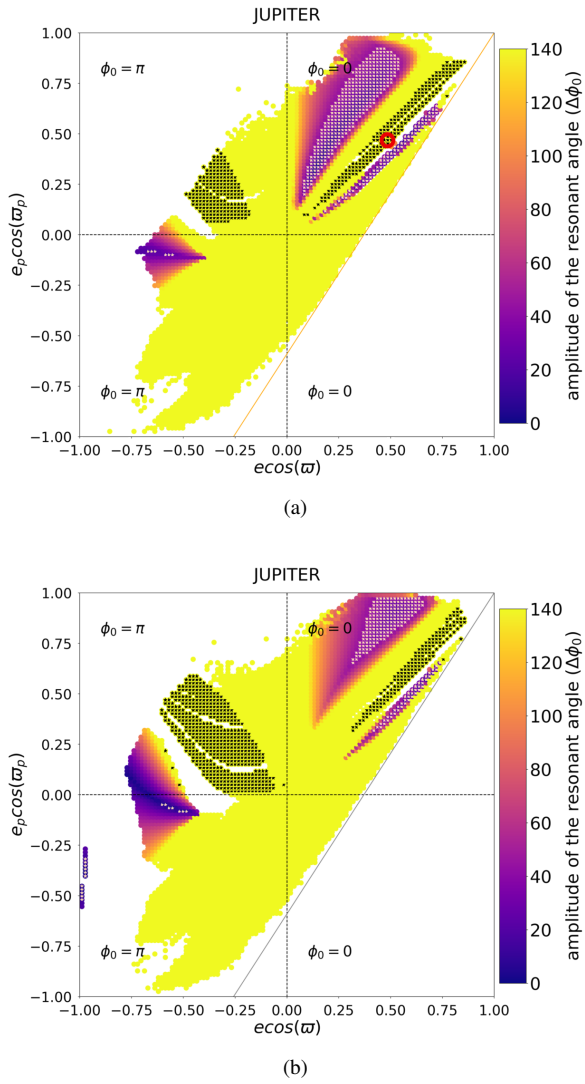


Figure 6. Resonant maps for the 1/2 resonance region considering the third body with Jupiter’s mass (a) $M = 0$; (b) $M = \pi$. The color bar represents the amplitude of the restricted angle (ϕ_0) and the overlaying points are the fixed point resonant where all resonant angles defined in this region librates around a center. The black symbol represents the libration of ϕ_3 . The orange and gray lines indicate collision at time zero or after half a period of the external object, respectively.

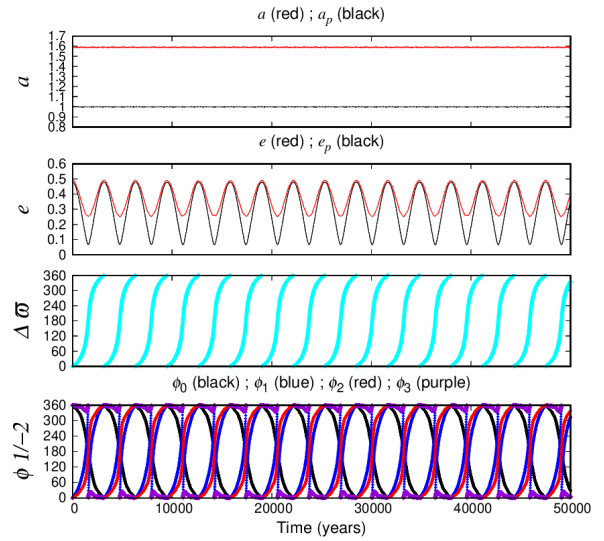


Figure 7. Orbital evolution as a function of time for the initial conditions circled in Figure 6a (Q_1 , $M = 0$). The initial conditions are $e = 0.49$, $e_p = 0.48$. The 1st panel shows the semi-major axes of both planets, the 2nd panel shows their eccentricities, the 3rd panel shows the difference Δw between the longitudes of pericenter, the 4th panel shows the resonant angles ϕ_0 , ϕ_1 , ϕ_2 , and ϕ_3 .

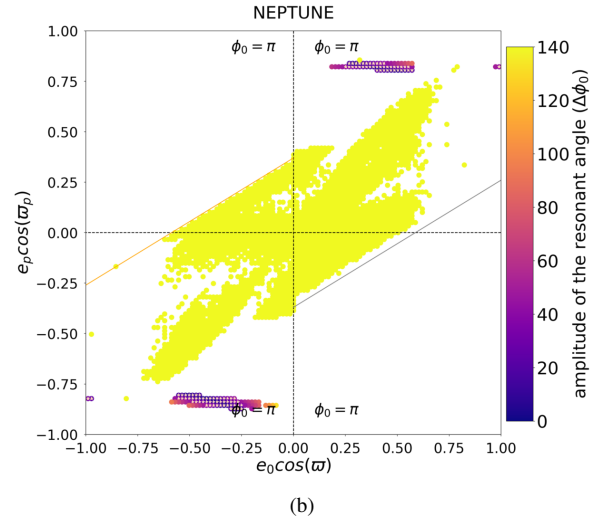
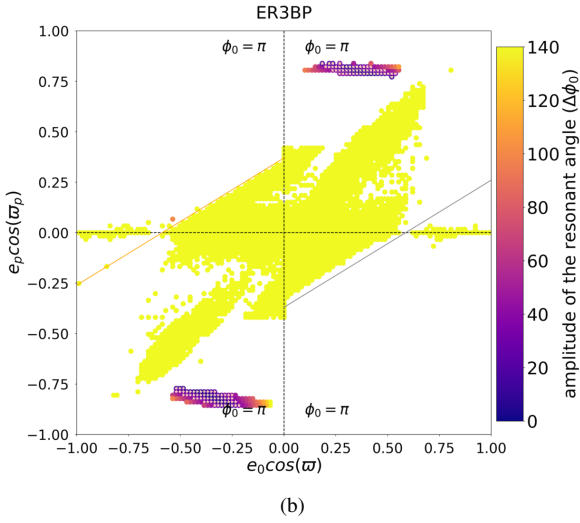
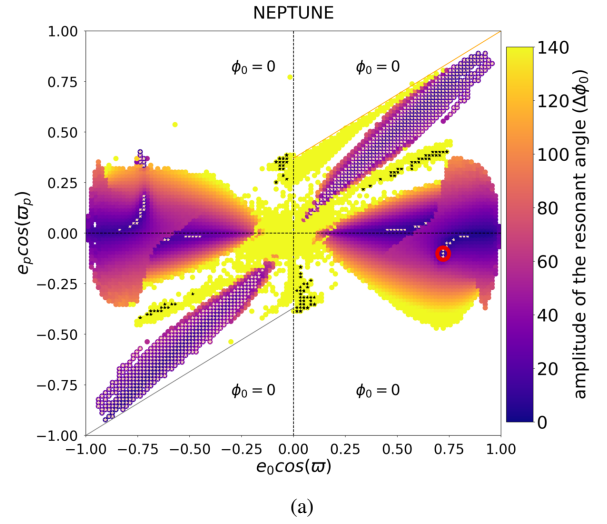
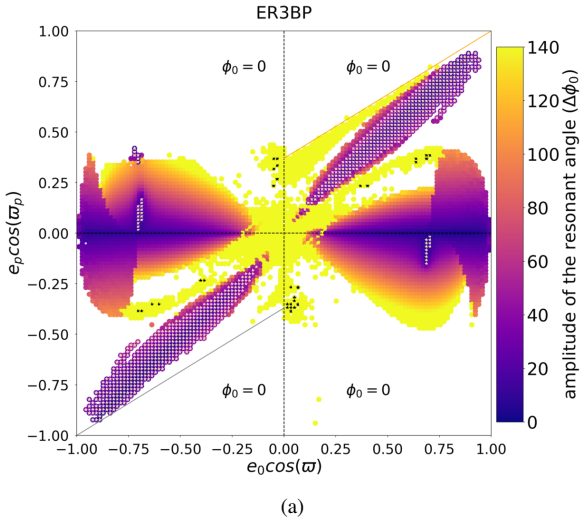


Figure 8. Resonant maps for the 2/-1 resonance in the elliptic restricted three body problem (a) $M = 0$; (b) $M = \pi$. The color bar represents the amplitude of the restricted angle (ϕ_0) and the overlaying white symbols indicate the fixed point family where all resonant angles librate around a center. The black symbol represents the libration of ϕ_3 . The orange and gray lines indicate collision at time zero or after half a period of the external object, respectively.

Figure 9. Resonant maps for the 2/-1 resonance in the planetary problem when the 2nd planet has Neptune's mass (a) $M = 0$; (b) $M = \pi$. The color bar represents the amplitude of the restricted angle (ϕ_0) and the overlaying white symbols indicate the fixed point family where all resonant angles librate around a center. The black symbol represents the libration of ϕ_3 . The orange and gray lines indicate collision at time zero or after half a period of the external object, respectively.

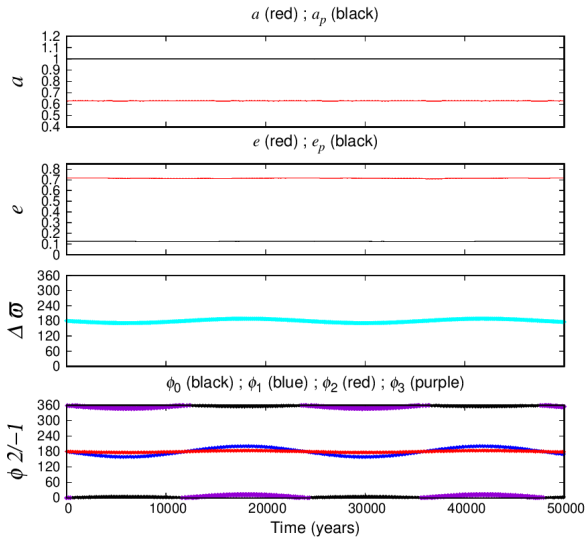


Figure 10. Orbital evolution as a function of time for the initial conditions circled in Figure 9a (Q_4 , $M = 0$). The initial conditions are $e = 0.718$, $e_p = 0.125$. The 1st panel shows the semi-major axes of both planets, the 2nd panel shows their eccentricities, the 3rd panel shows the the difference $\Delta\omega$ between the longitudes of pericenter, the 4th panel shows the resonant angles ϕ_0 , ϕ_1 , ϕ_2 , and ϕ_3 .

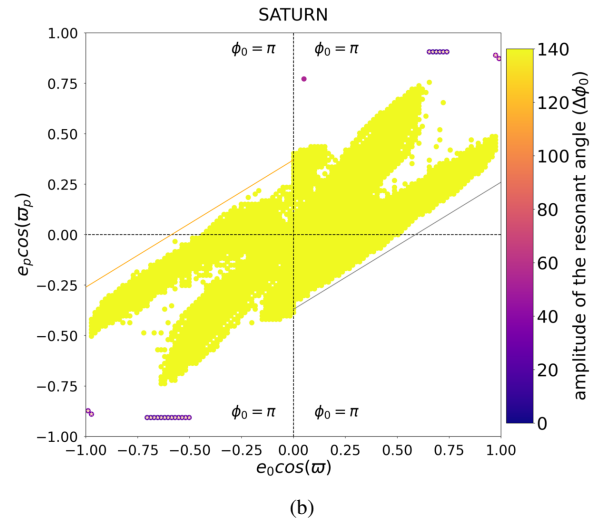
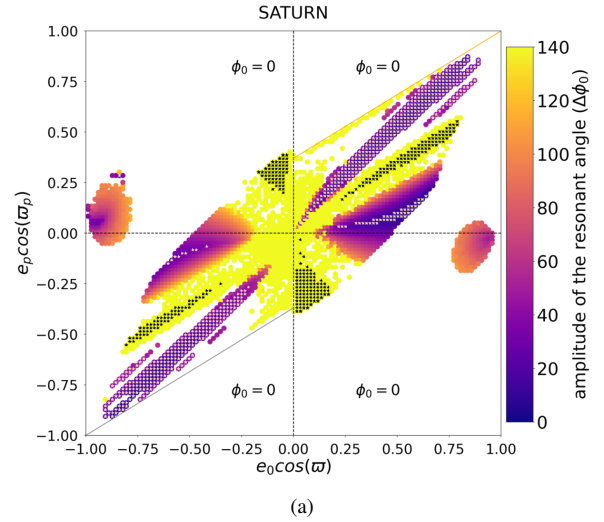


Figure 11. Resonant maps for the 2/-1 resonance in the planetary problem when the 2nd planet has Saturn's mass (a) $M = 0$; (b) $M = \pi$. The color bar represents the amplitude of the restricted angle ($\Delta\phi_0$) and the overlaying white symbols indicate the fixed point family where all resonant angles librate around a center. The black symbol represents the libration of ϕ_3 . The orange and gray line are the collision lines in $t = 0$ and $t = T_{ext}/2$ respectively.

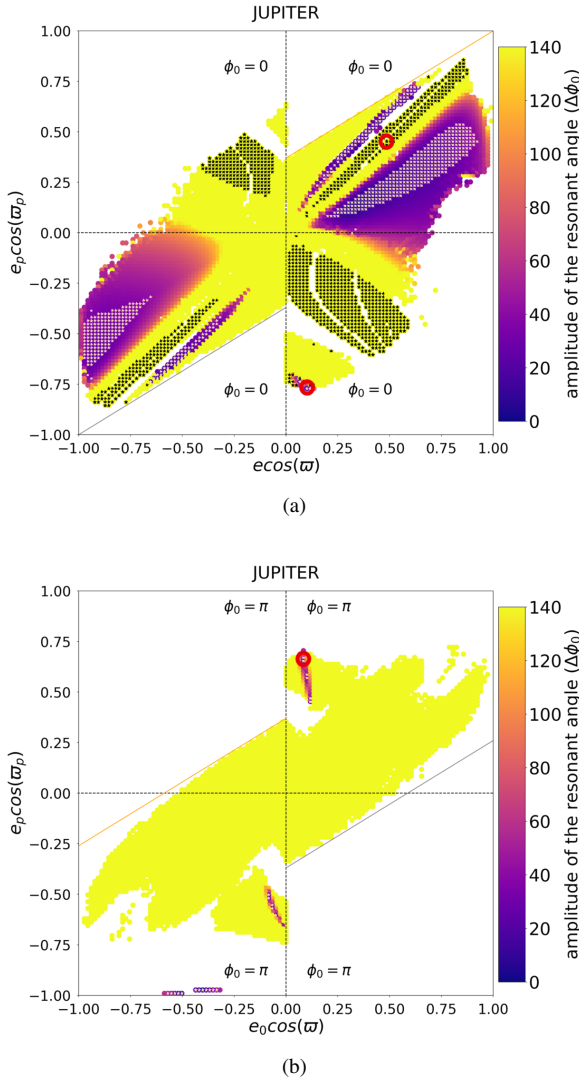


Figure 12. Resonant maps for the 2/-1 resonance in the planetary problem when the 2nd planet has Jupiter's mass (a) $M = 0$; (b) $M = \pi$. The color bar represents the amplitude of the restricted angle (ϕ_0) and the overlaying white symbols indicate the fixed point family where all resonant angles librate around a center. The black symbol represents the libration of ϕ_3 . The orange and gray lines indicate collision at time zero or after half a period of the external object, respectively.

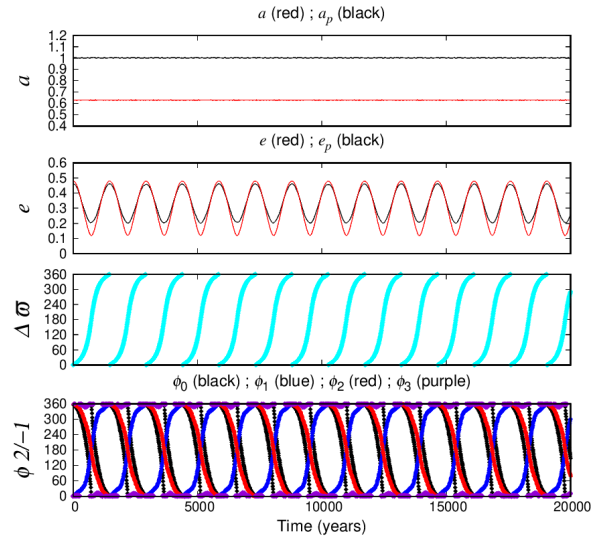


Figure 13. Orbital evolution as a function of time for the initial conditions circled in Figure 12a ($Q_1, M = 0$). The initial conditions are $e = 0.48$, $e_p = 0.46$. The 1st panel shows the semi-major axes of both planets, the 2nd panel shows their eccentricities, the 3rd panel shows the difference Δw between the longitudes of pericenter, the 4th panel shows the resonant angles ϕ_0, ϕ_1, ϕ_2 , and ϕ_3 .

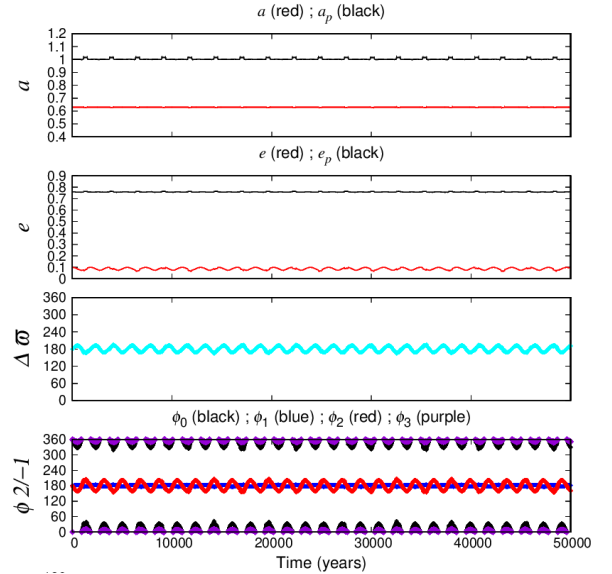


Figure 14. Orbital evolution as a function of time for the initial conditions circled in Figure 12a ($Q_4, M = 0$). The initial conditions are $e = 0.10$, $e_p = 0.76$. The 1st panel shows the semi-major axes of both planets, the 2nd panel shows their eccentricities, the 3rd panel shows the difference Δw between the longitudes of pericenter, the 4th panel shows the resonant angles ϕ_0, ϕ_1, ϕ_2 , and ϕ_3 .

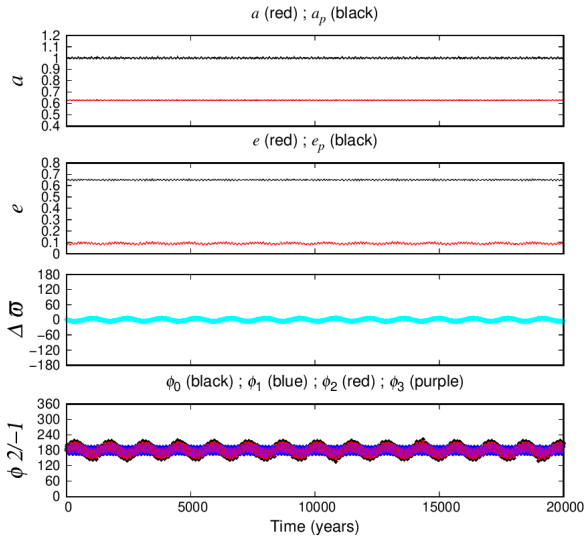


Figure 15. Orbital evolution as a function of time for the initial conditions circled in Figure 12b (Q_1 , $M = \pi$). The initial conditions are $e = 0.08$, $e_p = 0.65$. The 1st panel shows the semi-major axes of both planets, the 2nd panel shows their eccentricities, the 3rd panel shows the difference $\Delta\omega$ between the longitudes of pericenter, the 4th panel shows the resonant angles ϕ_0 , ϕ_1 , ϕ_2 , and ϕ_3 .

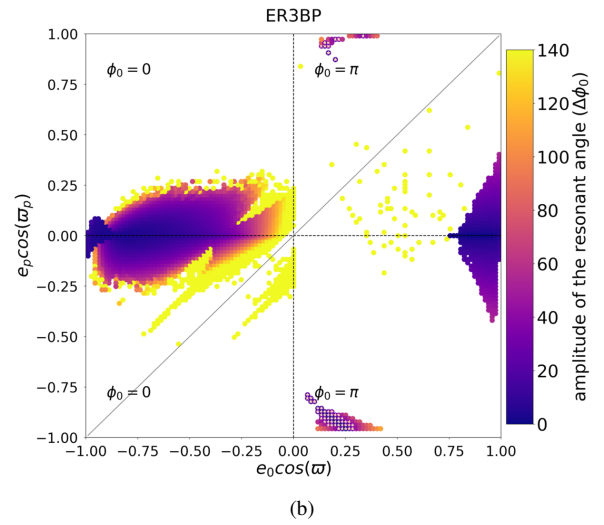
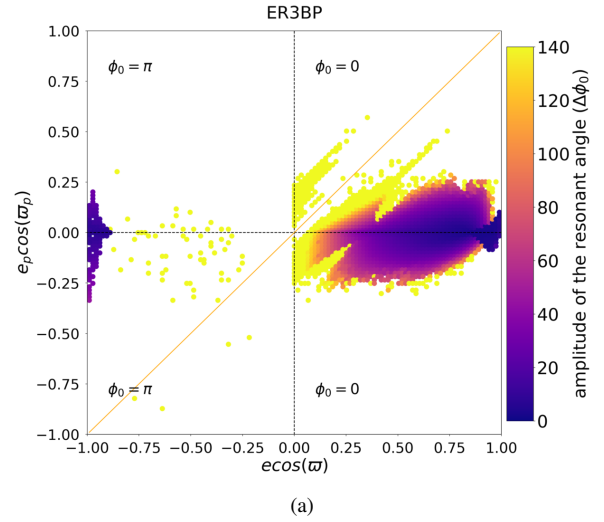


Figure 16. Resonant maps for the 1/-1 resonance in the elliptic restricted three body problem (a) $M = 0$; (b) $M = \pi$. The color bar represents the amplitude of the restricted angle (ϕ_0) and the overlaying white symbols indicate the fixed point family where all resonant angles librate around a center. The orange and gray lines indicate collision at time zero or after half a period of the external object, respectively.

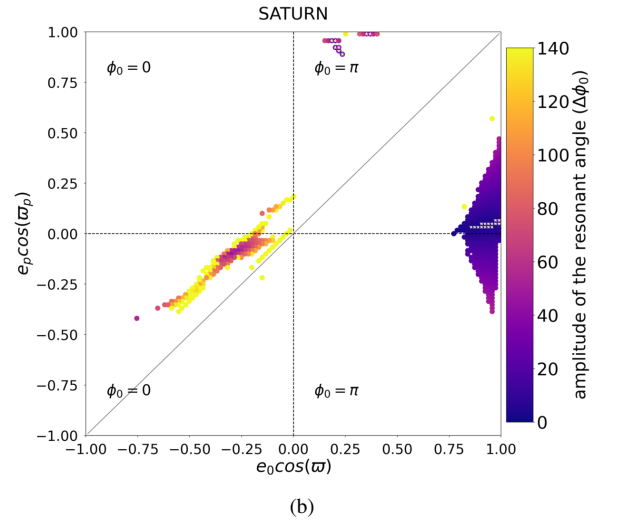
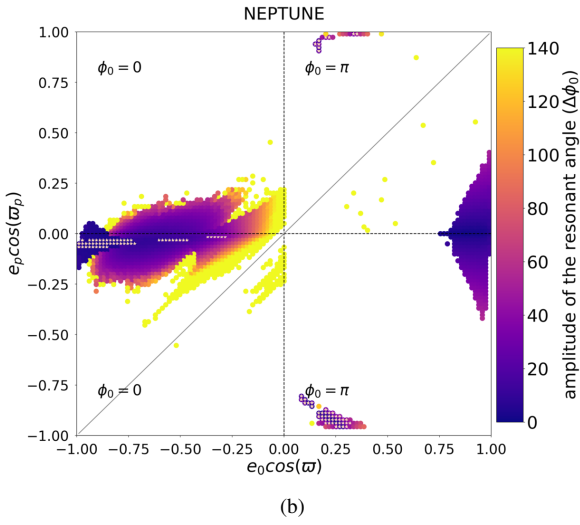
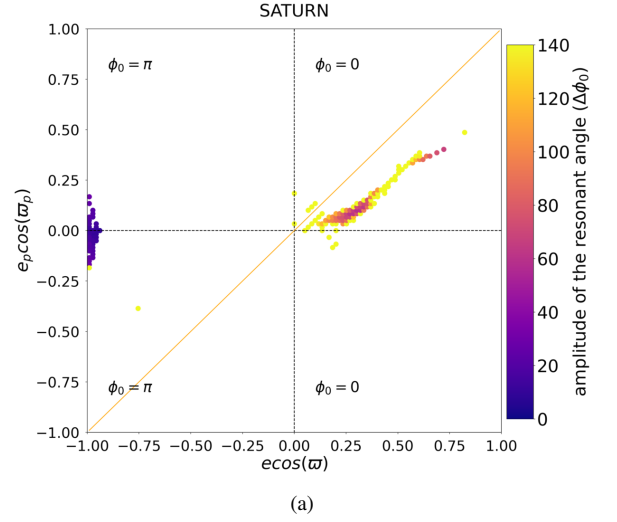
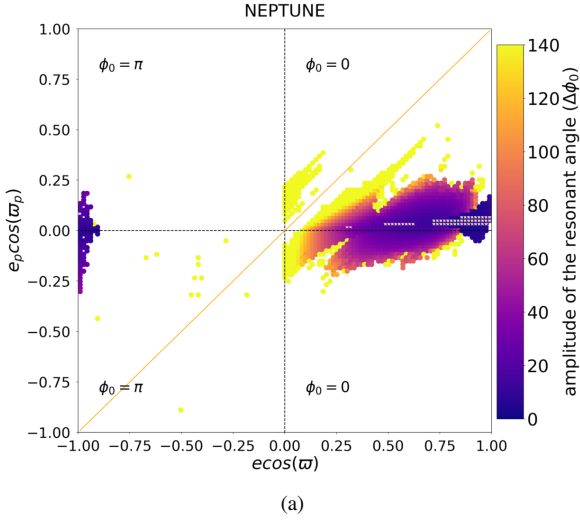


Figure 17. Resonant maps for the 1/-1 resonance in the planetary problem when the 2nd planet has Neptune’s mass (a) $M = 0$; (b) $M = \pi$. The color bar represents the amplitude of the restricted angle (ϕ_0) and the overlaying white symbols indicate the fixed point family where all resonant angles librate around a center. The orange and gray lines indicate collision at time zero or after half a period of the external object, respectively.

Figure 18. Resonant maps for the 1/-1 resonance in the planetary problem when the 2nd planet has Saturn’s mass (a) $M = 0$; (b) $M = \pi$. The color bar represents the amplitude of the restricted angle (ϕ_0) and the overlaying white symbols indicate the fixed point family where all resonant angles librate around a center. The orange and gray lines indicate collision at time zero or after half a period of the external object, respectively.

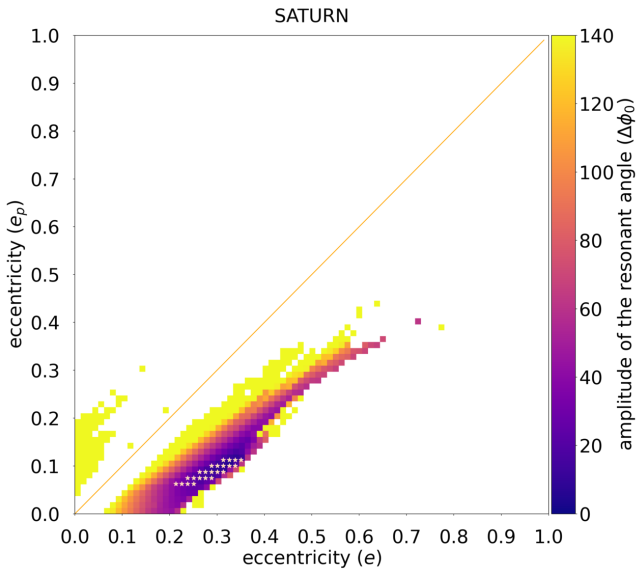


Figure 19. Resonant map for the 1/-1 resonance in the planetary problem when the 2nd planet has Saturn's mass with initial conditions and $a = 1.01$, $M = 0$, $\varpi = \varpi_p = 0$. The color bar represents the amplitude of the restricted angle (ϕ_0) and the overlaying white symbols indicate the fixed point family where all resonant angles librate around a center.

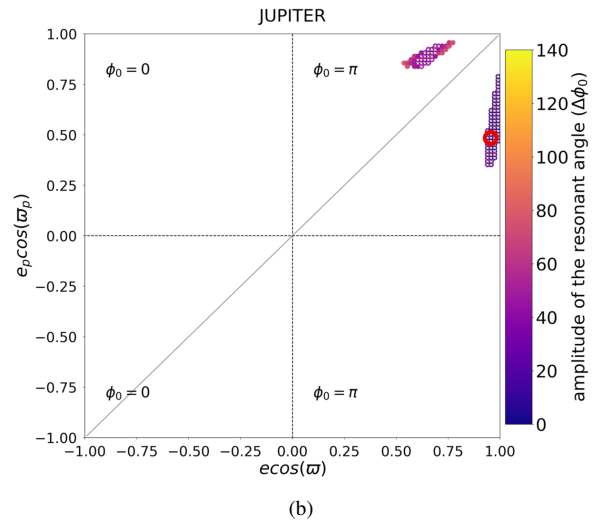
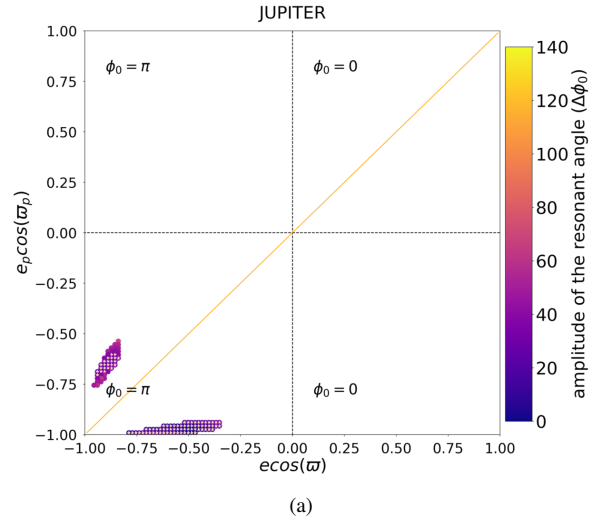


Figure 20. Resonant maps for the 1/-1 resonance in the planetary problem when the 2nd planet has Jupiter's mass (a) $M = 0$; (b) $M = \pi$. The color bar represents the amplitude of the restricted angle (ϕ_0) and the overlaying white symbols indicate the fixed point family where all resonant angles librate around a center. The orange and gray lines indicate collision at time zero or after half a period of the external object, respectively.

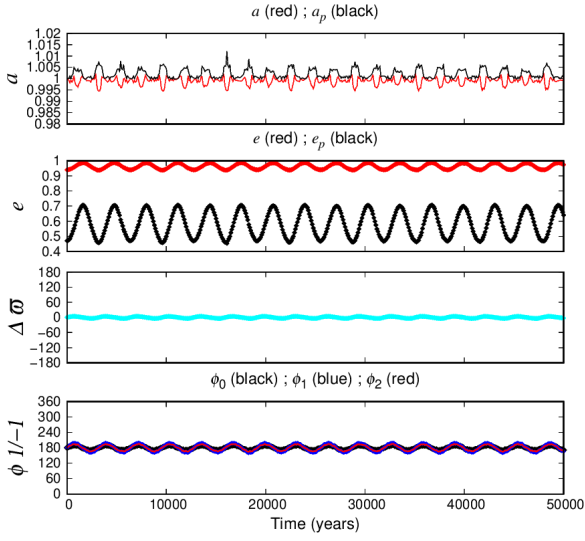


Figure 21. Orbital evolution as a function of time for the initial conditions circled in Figure 20b (Q_1 , $M = \pi$). The initial conditions are $e = 0.94$, $e_p = 0.47$. The 1st panel shows the semi-major axes of both planets, the 2nd panel shows their eccentricities, the 3rd panel shows the difference $\Delta\omega$ between the longitudes of pericenter, the 4th panel shows the resonant angles ϕ_0 , ϕ_1 and ϕ_2 .

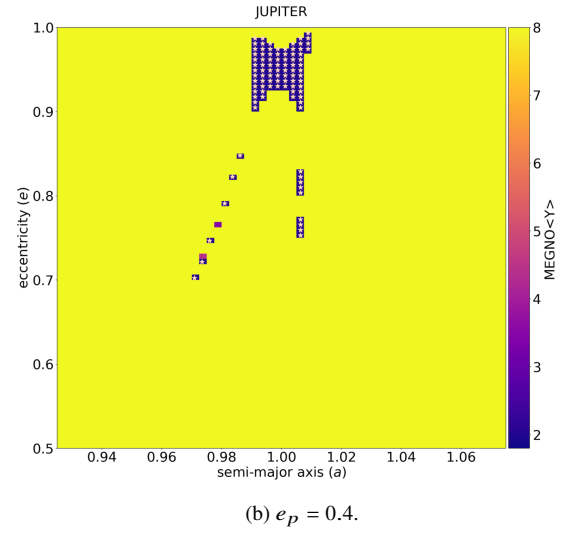
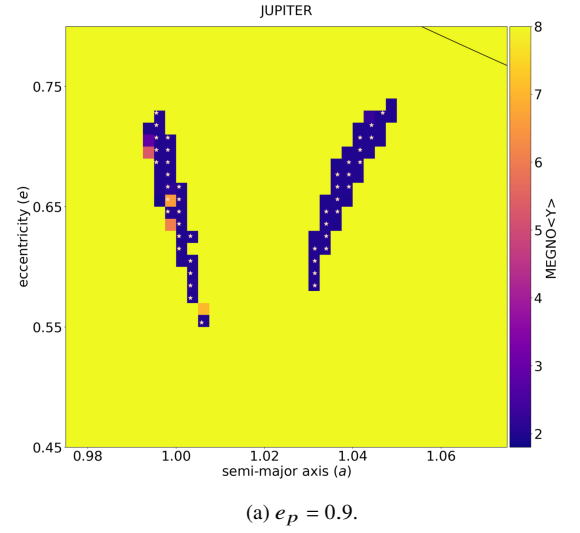


Figure 22. Stability map for resonance 1/-1 Jovian planetary system. The initial orbital elements adopted were $M = \pi$, $\omega = \omega_p = 0$. (a) $e_p = 0.9$ (40x40 grid); (b) $e_p = 0.4$ (8x80 grid). The color bar represents the MEGNO value. The black line represents the collision line.

3 DISCUSSION

In the planar CR3BP (Morais & Namouni 2013a, 2016a,b, 2019; Morais et al. 2021) the periodic orbits associated with the resonant families correspond to fixed resonant angle $\phi_0 = -q\lambda - p\lambda_p + (p + q)\varpi$ (Morais & Namouni 2013a), being either 0 or π , with ϖ circulating. We have seen here that in the ER3BP (non-zero eccentricity e_p) and in the planetary 3 body problem (2nd planet with non-zero mass) fixed point families of periodic orbits appear. Generally, as the mass ratio of the 2nd planet with respect to the 1st planet increases up to 1, the fixed point regions dominate the stable phase space. However, in the case of the 1/-2 and 2/-1 resonances, when the 2nd planet has Saturn's or Jupiter's mass, we saw that there are stable regions associated with libration of a mixed angle: $\phi_3 = -2\lambda - \lambda_p + \varpi_p + 2\varpi$ (1/-2); $\phi_3 = -\lambda - 2\lambda_p + 2\varpi_p + \varpi$ (2/-1). If we define the prograde planet to always be interior to the retrograde planet, then at the 2/-1 resonance $\phi_3 = -\lambda_p - 2\lambda + 2\varpi + \varpi_p$ which coincides with the definition of ϕ_3 at the 1/-2 resonance. This is expected since if the exterior planet is in the 1/-2 resonance with the interior planet, then the interior planet is in the 2/-1 resonance with the exterior planet, and the resonant argument is the same. As expected there is also exact symmetry between these configurations for the 1/-2 and 2/-1 resonances when the planets have identical masses.

Figure 23 shows periodic orbits of the planetary 3-body problem seen in the frame rotating with the prograde planet's true longitude angle, as defined in Hadjidemetriou & Voyatzis (2011). They have similar shapes to the periodic orbits of the CR3BP for these resonances, except for the variation of the prograde's planet orbit as it moves between pericenter and apocenter, represented by the blue line on the x-axis (Morais & Namouni 2013a, 2016a).

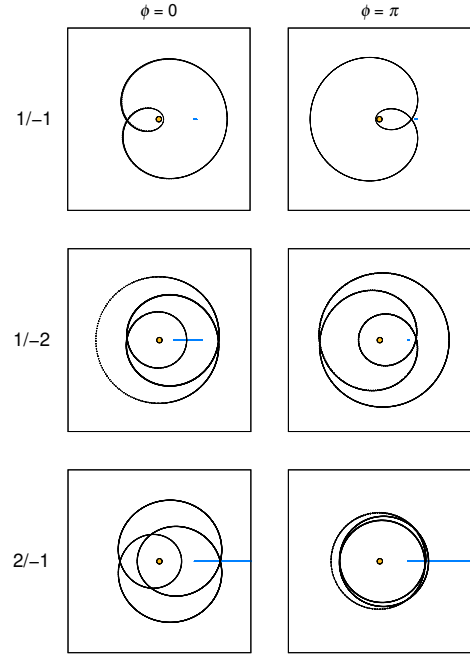


Figure 23. Orbits in synodic reference frame: 1/-1 (upper), 1/-2 (middle), 2/-1 (bottom) for $\phi = 0$ and π . The synodic orbit referred to the retrograde planet are represented in black. Except for the example of 2/-1 for $\phi = \pi$ which is obtained using Jupiter's mass, the others are obtained using the mass of Neptune. All examples chosen are fixed points taken from the maps of the three previous chapters. The blue line represents the prograde planet orbit in a synodic reference frame which moves on the x-axis when $e_p \neq 0$.

4 CONCLUSION

In this study we showed that there are stable configurations for the 1/2, 2/1 and 1/1 retrograde resonances in the planetary 3-body problem composed of a solar mass star, a Jupiter mass planet and a 2nd planet with either zero mass (ER3BP), or a non-zero mass equal to Neptune, Saturn or Jupiter. We saw that there are significant changes in the resonant phase space as we increase the mass ratio of the 2nd planet with respect to the 1st planet.

In general, in the case of a 2nd planet with Neptune's mass, there are no significant differences in stability with respect to the ER3BP, except for the appearance of additional fixed point families within the stable regions. As the mass of the 2nd planet increases the fixed point families become more predominant within the stable phase space. This happens for the 1/-2, 2/-1 and 1/-1 resonances.

The 1/1 retrograde resonance in the E3RBP has stable regions of quasi-periodic orbits associated with the CR3BP resonant centers $\phi_0 = 0$ and $\phi_0 = \pi$, and an additional family of fixed point periodic orbits appears at large eccentricity of the prograde planet, e_p . There are also stable retrograde coorbital configurations in the planetary 3-body problem. As the 2nd planet's mass increases, the $\phi_0 = 0$ center becomes less stable than the $\phi_0 = \pi$ center, which occurs at large e . In the case of 2 Jovian mass planets the stable regions correspond to fixed point periodic families with $\phi_0 = \pi$ and $\varpi - \varpi_p = 0$, that occur at large eccentricities.

The results presented in this article depend on the mass ratios and relative distances only hence may be applied to other systems. It has been proposed that counter revolving resonant planetary systems may exist around other stars (Gayon & Bois 2008; Gayon-Markt & Bois

2009). Our results show which stable configurations are possible and therefore may guide searches for such systems.

ACKNOWLEDGEMENTS

This work was funded by the Coordenação de Aperfeiçoamento de Pessoal de Nível Superior – Brasil (CAPES) – Finance Code 001. The authors acknowledge support from Grants FAPESP/2019/24958-5 & FAPESP/2021/11982-5 of São Paulo Research Foundation and from CNPQ-Brazil (PQ2/304037/2018-4). This work used computational resources supplied by the Center for Scientific Computing (NCC/GridUNESP) of the São Paulo State University (UNESP).

DATA AVAILABILITY

The data underlying this paper will be shared on reasonable request to the corresponding author.

REFERENCES

- Chambers J. E., 1999, *Monthly Notices of the Royal Astronomical Society*, 304, 793
- Cincotta P. M., Simó C., 2000, *Astronomy and Astrophysics Supplement Series*, 147, 205
- Dobrovolskis A. R., 2012, in *AAS/Division for Planetary Sciences Meeting Abstracts #44*. p. 112.22
- Gayon J., Bois E., 2008, *Astronomy & Astrophysics*, 482, 665
- Gayon-Markt J., Bois E., 2009, *Monthly Notices of the Royal Astronomical Society: Letters*, 399, L137
- Goździewski K., 2003, *Astronomy & Astrophysics*, 398, 1151
- Hadjidemetriou J. D., Voyatzis G., 2011, *Celestial Mechanics and Dynamical Astronomy*, 111, 179
- Kotoulas T., Voyatzis G., 2020a, *Celestial Mechanics and Dynamical Astronomy*, 132, 1
- Kotoulas T., Voyatzis G., 2020b, *Planetary and Space Science*, 182, 104846
- Kotoulas T., Voyatzis G., Morais M. H. M., 2022, *Planetary and Space Science*, 210, 105374
- Malmberg D., Davies M. B., Heggge D. C., 2011, *Monthly Notices of the Royal Astronomical Society*, 411, 859
- Morais M., Giuppone C., 2012, *Monthly Notices of the Royal Astronomical Society*, 424, 52
- Morais M., Namouni F., 2013a, *Celestial Mechanics and Dynamical Astronomy*, 117, 405
- Morais M., Namouni F., 2013b, *Monthly Notices of the Royal Astronomical Society: Letters*, 436, L30
- Morais M., Namouni F., 2016a, *Computational and Applied Mathematics*, 35, 881
- Morais M. H. M., Namouni F., 2016b, *Celestial Mechanics and Dynamical Astronomy*, 125, 91
- Morais H., Namouni F., 2017, *Nature*, 543, 635
- Morais M., Namouni F., 2019, *Monthly Notices of the Royal Astronomical Society*, 490, 3799
- Morais M., Namouni F., Voyatzis G., Kotoulas T., 2021, *Celestial Mechanics and Dynamical Astronomy*, 133, 1
- Namouni F., Morais M. H. M., 2015, *Monthly Notices of the Royal Astronomical Society*, 446, 1998
- Namouni F., Morais H., 2018, *Computational and Applied Mathematics*, 37, 65
- Rein H., Spiegel D. S., 2015, *Monthly Notices of the Royal Astronomical Society*, 446, 1424
- Wiegert P., Connors M., Veillet C., 2017, *Nature*, 543, 687

This paper has been typeset from a $\text{\TeX}/\text{\LaTeX}$ file prepared by the author.